Available online at www.derpharmachemica.com

ISSN 0975-413X
CODEN (USA): PCHHAX

Der PharmaChemica, 2016, 8(19):317-327
(http://derpharmachemica.com/archive.html)

Synthesis of Copper complexes of a new symmetrical dihydrazone: Characterization, XRD studies, DFT calculations and biological activity

O. A. El-Gammal[a]*, D. A. Saad[a,b] and A. A. El-Asmy[a,c]

[a]*Department of Chemistry, Faculty of Science, Mansoura University, Mansoura, P.O.Box 70, Mansoura- Egypt*
[b]*Northern Boarder University, Saudi Arabian Kingtodom*
[c]*Department of Chemistry, Faculty of Science, Kuwait University, Kuwait- AlAin*

ABSTRACT

A novel series of binuclear Cu(II) chelates of 2,2'-thiobis(N-benzylidene)acetohydrazide) (H_2L) obtained by the condensation of 2,2'-thiodi(acetohydrazide) with benzaldehyde was synthesized using different copper salts. The prepared copper complexes were identified by elemental analysis, spectral (IR, UV-visible, ESR, ^1H, $^{13}CNMR$ and mass), as well as magnetic and thermal measurements. The ligand behaves either as mono- or dibasic NNOO-tetradentate. The formulae:$[Cu_2(L\text{-}H)(OH)_2(C_2H_5O)(H_2O)]$, $[Cu_2(L\text{-}2H)(L\text{-}H)(OAC)(H_2O)].4H_2O$, $[Cu_2(L\text{-}H)_2(NO_3)_2].2H_2O$ and $[Cu_2(L\text{-}2H)SO_4(H_2O)_3]H_2O.1/2C_2H_5OH$ were suggested for the newly synthesized complexes.On the premise of their electronic spectra and magnetic moments data; square planner, square pyramidal and octahedral geometries were proposed for the complexes. Details of the chemical constitution of the $[Cu_2(L\text{-}H)(OH)_2(C_2H_5O)(H_2O)]$complex were obtained from X-ray powder diffraction data. The geometries of all investigated compounds were further affirmed by DFT calculations. Moreover, the synthesized compounds were examined for their antibacterial and superoxide dismutase (SOD)-like activities.

Keywords: Hydrazone; transition metal complexes; spectral characterization; thermal decomposition; antibacterial and anti-oxidant activities.

INTRODUCTION

Hydrazones have been extensively studied for many decades due to their synthetic flexibility and selectivity as well as their high affinity to the transition metal ions[1,2].The design excellence of their coordination edifices emerges from the inclusion of different donor sites, such as, NNO in their chemical constitution. Hydrazonesact mostly as bi-/tri- or tetradentate ligands[3-9], although they have the potential to act as bridging tetradentate ligands, especially, dihydrazones which are potential polyfunctional ligands [10-16] capable of exhibiting (keto – enol) tautomerism. Generally, the transition metal complexes display extensive variety of fascinating chemical, physical, and biological features, which find valuable applications in polymer industry[17], pharmaceuticals[18,19], catalysis[20], and molecular sensors[21].

Driven by their distinguished chemical, biological, and magnetic properties, synthesis and characterization of copper complexes, continue to be a very active area of research. In fact a variety of Cu(II) complexes are well-known for their cytotoxic [22], antimicrobial[23], antibacterial[24,25] and anticancer activities[26].

In view of the aforementioned facts, we are highly interested in the synthesis of 2,2'-thiobis(*N*-(benzylidene)acetohydrazide) (H_2L) as a novel dihydrazone ligand and studying its behavior towards different Cu(II) salts.

MATERIALS AND METHODS

2.1 Materials and physical measurements.

chemicals used were of analytical grade and purified prior to use unless otherwise stated. Elemental analyses (C, H and N)were performed with a Perkin-Elmer 2400 series II analyzer. C,H,N,Cl and metal content were preformed according to the standard methods.IR spectra (4000–400cm^{-1}) for KBr discs were recorded on a Mattson 5000 FTIR spectrophotometer. Electronic spectra were recorded on a Unicam UV–Vis spectrophotometer UV2. Magnetic susceptibilities were measured with a Sherwood scientific magnetic susceptibility balance at 298 K. NMR spectra were measured using Varian Vnmr 400 (^{1}H, 400 MHz; ^{13}C, 101 MHz) spectrometer using $CDCl_3$, or DMSO-d_6 as a solvent and internal reference. Electrospray ionization (ESI) mass spectra were recorded on a Thermo Scientific (Rockford, IL, USA) Q Exactive (Orbitrap mass spectrometer). Thermo-gravimetric measurements (TGA, DTA, 20–800˚C)were recorded on a DTG-50 Shimadzu thermogravimetric analyzer at a heating rate of 10 °C/min and nitrogen flow rate of 15 ml/min. A powder ESR spectrum was carried out in a 2 mm quartz capillary at room temperature with a Bruker EMX spectrometer working in the X-band (9.78 GHz) with 100 kHz modulation frequency. XRD patterns were obtained using Philips X-ray diffractometer (model X'pert) with utilized monochromatic CuKa radiation operated at 40 kV and 30 mA and a scanning speed of 8 (deg/min) in the 2θ range 10°–80°.

2.2.Synthesis of 2,2'-thiobis(N-benzylidene)acetohydrazide)(H_2TBAH)

2,2'-thiodi(acetohydrazide) (TAH) was synthesized as prescribed previously [27].To a stirred solution of 2,2'-thiodi(acetohydrazide) (1.78 g, 0.01 mol)in water (20 ml), a solution of benzaldhyde (2.653 g, 2.54 ml, 0.025 mol) was added in ethanol (50 ml), within few minutes, the solution become hazy and a white precipitate formed. Stirring was continued at room temperature for 1 hour, and the formed precipitate was filtered off, washed with water and cold ethanol, air dried and recrystallized from ethanol. The purity of the hydrazone (H_2L) was checked by TLC, m.p:150 °C; yield (3.05 g, 86%); IR (KBr) υ/cm^{-1}:3450, 3435 (w, ν(OH)), 3239, 3210(m, ν(NH)), 1668(s,ν(C=O)), 1605(s,$\nu(C=C)_{ph}$), 1551ν (C=N)$_{azo}$), 1176(s, ν(C-O)), 1063(s, ν(N-N)),690(s,ν(C-S)); ^{1}H NMR (400 MHz, dmso) δ 11.57 (d, *J* = 11.3 Hz, 1H), 11.47 (d, *J* = 16.1 Hz, 1H), 8.18 (d, *J* = 5.5 Hz, 1H), 7.98 (d, *J* = 12.6 Hz, 1H), 7.73 – 7.57 (m, 4H), 7.48 – 7.32 (m, 6H), 3.82(dd, *J* = 14.4, 1.5 Hz, 2H), 3.44 – 3.36 ppm (m, 2H); ^{13}C NMR (101 MHz, dmso) δ 170.68, 170.53, 143.28, 143.15, 134.13, 134.10, 130.03, 129.81, 129.77, 128.76, 128.74, 127.05, 126.81, 126.76, 32.51, 32.11ppm; MS (ESI) *m/z* = 355.1 (M^+ + H).

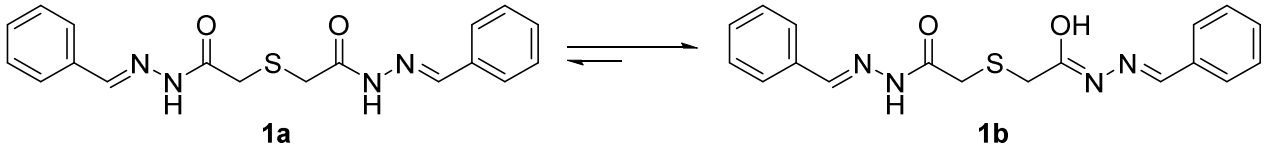

Structure 1: 2,2'-thiobis(N-benzylidene)acetohydrazide (H_2L)

2.3. Synthesis of metal complexes

Hot ethanolic solution (20 ml) of the coppersalts (acetate, chloride, nitrate and sulphate) (0.001 mol) was added to a hotethanolic suspension (20 ml) of the respective ligand (0.001 mol) with constant stirring. A precipitate was formed immediately and the reaction mixture was refluxed with constant stirring for 2hours at 100°C. The complexes were filtered, washed several times with hot ethanol and dried under vacuum anhydrous $CaCl_2$. The physical and analytical data are listed in (Table 1).

2.4. Computational details

Molecular Modeling

To examine the cluster estimations ,All calculations were carried out using DMOL3 module [28] and double numerical basis sets plus polarization functional (DNP) implemented in Materials Studio bundle [29]. DNP basis sets amounting to 6-31G Gaussian premise sets [30]. While, It was considered before, by Delley et al [31] that Gaussian premise sets are less precise than the DNP premise sets of similar size. The RPBE practical is utilized to take record of the trade and relationship impacts of electrons, where it is so far considered the best exchange–correlation utilitarian [32], based on the generalized gradient approximation (GGA) [33]. The geometric optimization displayed without any symmetry limitation.

2.5. Biological studies

2.5.1. Antimicrobial activity

The prepared compounds were tested for their antimicrobial activity against *Staphylococcus epidermidis(St. epid) and Streptococcus pyagenies(Strppy.),* as Gram-positive bacteria, *and Erwinia(Er.)klebsiella Spp* (kleb. spp.), as

Gram-negative bacteria, by the hole plate diffusion method [34], and using ampicillin as a reference. The experimental procedures for studying the antimicrobial activity were the same as described previously. [35]

2.5.2.Superoxide dismutase (SOD)scavenging activity

Superoxide dismutase (SOD)-like activity was tested using Bridges and Salin method [36]. This method is used on the basis of the inhibitory action of SOD on the reduction of nitrobluetetrazolium (NBT) by the superoxide anion produced by the xanthine/xanthine oxidase system. Free (H_2L) ligand solution or its copper complexes were prepared in dimethylsulphoxide (DMSO). For comparative intents, the activity of *L-Ascorbic acid* has also been determined.

RESULTS AND DISCUSSION

The complexes are insoluble either in water or in non-polar organic solvents but soluble in DMF and DMSO solvents. The molar conductivity of all complexes in DMSO lie in the range (8-19 ohm^{-1} cm^2 mol^{-1}) revealing their non-electrolytic nature [37]. Regrettably, we couldn't grow up single crystals for the solid metal complexes.

3.1 IR spectral studies.

The IR spectral data of investigated compounds are listed in (table 2). The spectrum of H_2L (Structure1) showed two sharp bands at 1668 and 1551cm^{-1} attributable to ν(C=O) and $\nu(C=N)_{azomethine}$ modes, respectively. The band due to $\nu(C=N)_{azomethine}$ vibration shifts to lower wavenumber upon complexation. The medium band observed at 1605 cm^{-1}isassigned to $\nu(C=C)_{ph}$. The medium intensity band at 1063 cm^{-1} is attributed to ν(N-N), while the bands at 3210 and 3229 $cm^{-1}$are assigned to ν(NH) vibrations of hydrazone moiety as well as N-H from ketone-type acylhydrazone (-O=C-N-N=C-), respectively deformation modes[38, 39].The previous assumption was further confirmed by the molecular modeling of H_2L as the two isomers possessed nearly equal binding energy (-4794.61, -48014.72 kcal/mol) for keto and enol isomers, respectively. The higher value of the enol form compared to that of the keto form indicates the higher stability. H_2L behaves in either mono- or binegative NNOO tetra-dentate manner depending upon the metal salt used.

H_2L acts as monobasic tetradentate on coordination to two copper atoms in $[Cu_2(L\text{-}H)(OH)_2(C_2H_5O)(H_2O)]$ and $[Cu_2(L\text{-}H)_2(NO_3)_2]2H_2O$. The chelating occurred via oxygen atoms of (C=O) in either keto and enol form (C-OH) and two $(C=N)_{azomethine}$ groups. This mode of chelation is confirmed by the shift of bands due to these groups to lower wavenumber. The shift of *ν* (N-N) mode to higher and lower wavenumbers respectively, is a further evidence for the coordination via the azomethine nitrogen.

From the infrared spectra of the nitrato complexes, data with respect to the conceivable bonding modes of the nitrate group was obtained. The bands at 1460 and 1315 cm^{-1} are due to respectively *ν*(N=O) (ν_1) and $\nu_{as}(NO_2)(\nu_5)$ of the coordinated nitrate. Additionally, $\nu_s(NO_2)(\nu_2)$ is notable at 1029 cm^{-1} that are characteristic of bidentate chelating nitrate with frequency separation, $\Delta\nu = \nu_1\text{-}\nu_5$ [40].

In $[Cu_2(L\text{-}H)(L\text{-}2H)(OAc)(H_2O)].4H_2O$ complex, one ligand molecule binds as mononegative-tetradentate towards two copper atoms via one C-O, one C=O and two $C=N_{azomethine}$from one side and the other molecule as binegative tetradentate coordinating both copper atoms from other side via two C-O and two azomethine groups. This mode is confirmed by: i) the change in intensity with shift of ν(C=O) mode to lower wavenumber. ii) the weakness of the band due to ν(NH) with the appearance of two new bands at 1543 and 1131 cm^{-1}assigned to new ν(C=N*) and ν(C-O) suggest that one carbonyl group undergoes enolization followed by deprotonation. iii) lowering in the C=N energy on complexation is in accordance with the coordination of the imine nitrogen, iv) increase of the frequency of ν(N-N) is due to the increase in the bond strength confirming the coordination via the azomethine nitrogen and v) the broad band appeared at 1553 cm^{-1} which may be considered as an overlap of ν(C=N)* with ν_{as}(OCO) and 1447 cm^{-1} assignable to ν_s(OCO) affording wave number separation value (Δ = 199 cm^{-1}) characteristic of monodentate acetate anion [41]. In $[Cu_2(L\text{-}2H)SO_4(H_2O)_3]H_2O.1/2C_2H_5OH$, H_2L binds via two enolized C-O and two azomethine groups as supported by weakness of the bands attributed to ν(NH) modes. The appearance of new bands at 3423, 1547 and 1113cm^{-1} assignable to ν(OH), ν(C=N)* and ν(C-O) vibrations. The bands located at 1229, 1040, 960 and 464 cm-1 are due to ν_3 ,ν_1, ν_4 and ν_2 modes of the sulphate ion suggesting its bidentate nature [42]. Also, the new bands in the IR spectra of all complexes in the region 561-509 and 474-424 cm^{-1} assignable to ν(M-O) and ν(M-N), respectively[43]. Finally, the broad bands at ≈ 3423-3438, 869-850, and ≈ 554cm^{-1}in the IR spectra of the investigated complexes are referred to ν(H_2O), $\rho_r(H_2O)$ and ρ_w (H_2O) for the coordinated water [43]. The broad band centered at ≈ 3500 cm^{-1} in the spectra of the studied complexes may be due to the hydrated water. Coordinated and hydrated water in metal complexes and be diffrentiated using TGA measurement.

3.2.^{1}HNMR and ^{13}CNMR spectra

The ^{1}HNMR spectrum of the ligand H_2L in DMSO-d_6, revealed its existence as a mixture of the two tautomeric forms,**1a** and **1b**, in 22 and 78 percentages respectively. Where the chemical shifts characteristic to the keto form (**1a**) appeared at, 11.45 (NH), 7.98 (azomethine protons), and 3.82 ppm (-$COCH_2$-S- protons).While the presence of the form **1b** was revealed by the appearance of another downfield proton at 11.57 (C(OH)=N proton), a more deshielded azomethine proton at 8.18, and a more shielded S-CH_2 group at 3.4 ppm. Whereas, the aromatic protons appeared as two multiplets at 7.38 and 7.65 ppm. Furthermore, the appearance of two signals at 170.58 (C(OH)=N carbon) and 170.53 (C=O, carbon) ppm, in addition to the duplication of the other signals in the ^{13}C spectrum of the ligand H_2TBAH, give a great support to the tautomerisation of H_2TBAH in solutions.

3.3.Electronic spectra and magnetic moments

The UV-Vis spectral study of H_2TBAH and its Cu(II) were carried out in dimethylformamid (DMF) solution or Nujol mull. No disparity was seen for peaks in case of the two solvents. The provisional assignments of the significant spectral absorption bands and magnetic moments of metal complexes are given in (Table 3).The electronic spectrum of H_2L shows an absorption band at 280 nm (35714 cm^{-1}) assignable to $\pi \rightarrow \pi^*$ transition of (C=C) of benzene rings. A red shift is observed for this transition in the spectra of complexes as a result of coordination of the azomethine. An intense absorption band observed at 310nm (32258 cm^{-1}) attributed to $\pi \rightarrow \pi^*$ of azomethine and carbonyl groups which shift in complexes toward higher frequencies, supporting the coordination of the azomethine nitrogen and carbonyl oxygen atoms with the central metal ion. The band at 25510 cm^{-1}appointed to ($n\rightarrow\pi^*$) of the carbonyl group [35].

The electronic spectrum of$[Cu_2(L\text{-}H)(OH)_2(C_2H_5O)(H_2O)]$complex exhibits two bands: an asymmetric broad band at 560 nm (17857 cm^{-1}) assignable to d-d transitions of the metal ions ($^{2}B_{1g}\rightarrow{}^{2}E_g$) which strongly favour square-planar geometry around the central metal ion [44] and a more intense band at 442 nm (22624 cm^{-1}). The latter band may be attributed to ligand metal charge transfer transition. The spectrum of $[Cu_2(L\text{-}H)_2(NO_3)_2].2H_2O$ complex shows two bands, one at 502 nm (19920 cm^{-1}) with a shoulder on the low energy side at ≈552 nm (18115 cm^{-1}) due to $^{2}B_{1g}\rightarrow{}^{2}E_g$ and $^{2}B_{1g}\rightarrow{}^{2}A_{1g}$ transitions, respectively, in an octahedral geometry [45] .

The spectrum of $[Cu_2(L\text{-}H)(L\text{-}2H)(OAc)(H_2O)].4H_2O$ in Nujol mull shows one low-energy band at 15150 cm-1 which is typically expected for square pyramidal geometry [46]. For these complexes, intense bands at (22831 - 24038) and 27777 cm^{-1} may be due to O→ Cu and N→ Cu charge transfer transitions [45]. Above aforementioned complexes, they are no doubt binuclear in nature, they exhibit abnormal magnetic moment value per one metal atom referred to the strong Cu-Cu interaction[47].

3.4.Electron spin resonance

The X-band ESR spectrum of $[Cu_2(L\text{-}H)_2(NO_3)_2]2H_2O$ as a representative example was recorded in the solid state at room temperature and is shown in Fig.1. The spectrum showed an intense broad signal and subsequently, one g value emerges from broad exchange coupling through misalignment of the local molecular axes between different molecules in the unit cell (dipolar broadening) and enhanced spin lattice relaxation [48] without hyperfine splitting (g_{iso} = 2.075). This is presumably because of insufficient spin-exchange narrowing toward the coherence of four copper hyperfine lines to a single line. Similar kind of powder ESR line shapes; have also been observed for many binuclear octahedral Cu (II) complexes possess a strong spin-exchange interaction [49]. This assumption was further confirmed by the low magnetic moment value ($\mu_{eff.}$=1.67 B.M). The higher g value for the investigated complex, compared to that of free electron (g= 2.0023), suggested an appreciable covalency of the metal ligand bonding with d_{x2-y2} as the ground-state feature of octahedral geometry [50].

3.5. Thermogravimetric studies.

The structural elucidation of the investigated complexes was further recognized by a careful examination of their thermogravimetric, TG patterns. The data obtained listed in (Table 4) revealed a good matchmaking between the chemical composition and the fragmentation pattern.TG of the ligand represented three decomposition stages while its metal complexes represented four, five or sex decomposition stages. The first degradation stage in metal complexes generally occurred before 150^{o} presumably due to loss of hydrated water and/or ethanol molecule. The following decomposition stages that started later continued until the complete decomposition of the molecule ultimately leaving either the metal sulfide or the metal oxide as the residue.

3.6.X-ray powder diffraction studies

X-ray powder diffraction analysis was carried out in order to obtain further evidence about the structure of the complex. The average crystallite size D and ε- lattice strain was calculate using Scherrer and Williamson–Hall equations.

$$D = \frac{k\lambda}{\beta \cos\theta} \ , \quad \varepsilon = \beta \frac{cos\theta}{4sin\theta} - \frac{k\lambda}{4Dsin\theta} \qquad (1)$$

where λ is the X-ray wavelength = 1.54606(A°), κ a constant of nearly 0.94, β the full width at half maximum intensity(FWHM) in radians and θ the Bragg angel.
The X- ray diffraction pattern of $[Cu_2(L\text{- }H)(OH)_2(C_2H_5O)(H_2O)]$ is shown in (fig 2). The calculated values of interplaner d-spacing, crystallite size (D) and lattice strain (ε) along with 2θ, FWHM and intensity (%) are summarized in table (5).

The complexhas the crystallite size of average 40.09 nm. It represents the mean size of every Nano crystallite complexes.

3.7. DFT molecular modeling.
The optimized molecular structure of Copper complexes along with atom numbering are shown in structures (2 to 4).

From bond lengths and bond angels calculated data, the following remarks can be concluded;
i. The bond angles of the hydrazone moiety of H_2TBAHwere changed slightly upon coordination; the largest change affects in H_2TBAH are C(15)-C(13)-N(11), C(14)-C(12)-N(10),H(33)-C(13)-N(11),H(32)-C(12)-N(10), C(15)-C(13)-N(11), C(14)-C(12)-N(10), C(13)-N(11)-N(7), C(12)-N(10)-N(6), N(11)-N(7)-C(5), N(10)-N(6)-C(4), O(9)-C(5)-N(7), O(8)-C(4)-N(6), O(9)-C(5)-C(1), O(8)-C(4)-C(3)angles. The bond angles in the H_2TBAH are changed upon complexation as a result of bonding with metal ion[51].

ii. The bond angles are fairly consistent with an octahedral and square pyramidal geometry expectingsp^3d^2 hybridization in $[Cu_2(L\text{-}H)_2(NO_3)_2].2H_2O$ and$[Cu_2(L\text{-}2H)(L\text{-}H)(OAC)(H_2O)]4H_2O$, respectively. Moreover, $[Cu_2(L\text{- }H)(OH)_2(C_2H_5O)(H_2O)]$ afforded square planner geometry with dsp^2 hybridization.

iii. C(3)-S(2)-C(1) angel in free ligand was noted to be changed to higher value in consequence of coordination.
iv. All the active groups that participate in chelation with Cu(II) ion have bonds lengthy compare with ligand as (C=O), (C-OH), $(C=N)_{azomethine}$, indicating the formation of M-N and M-O bonds which results in weakness of C-N bond as the effect of coordination via N atom of $(C=N)_{azomethine}$, (C=O) and (C-OH)[52].

v. The complexation made the bond lengths of C(13)-N(11) and C(12)-N(10) longer than of H_2TBAH in caseof $[Cu_2(L\text{-}2H)(L\text{-}H)(OAC)(H_2O)]4H_2O$ and$[Cu_2(L\text{-}2H)SO_4(H_2O)_3]H_2O.1/2C_2H_5OH$ as the coordination occurred through N atom of -C=N-N=C- group in the enolized ligand. While in case of $[Cu_2(L\text{-}H)_2(NO_3)_2]2H_2O$ and $[Cu_2(L\text{-}H)(OH)_2(C_2H_5O)(H_2O)]$ one bond showed slightly higher value but the other unchanged which provided the existence of ligand in keto-enol form. That is referred to the formation of M-N bond as a result of coordination via N atom of azomethane group$(C=N)_{az}$[52].

vi. C(5)-C(O9) and C(4)-O(8) bond lengths in H_2TBAH was changed to higher extent after coordination through deprotonated -C-OH group whereas in case of the ligand in keto form (-C=O), the bond length was either unaltered or decreased somewhat.vii. The bond angels of ligand moiety holding donor centres will be varied in all particular compounds due to the formation of N-M-O chelate ring[53].viii. According to the order of $M\text{-}N_{azomethine}$ and $M\text{-}O_{carbonyl}$ bond lengths, the data displayed slightly higher strength of the Cu-N rather than Cu-O bonds. ix. The energy values of both HOMO (π donor) and LUMO (π acceptor) are important parameters in quantum calculations Fig.3.

In many reactions, the nearby belong to HOMO and LUMO orbitals considered as a control factor, where in H_2TBAH; the orbitals of higher molecular coefficients can be counted as the basic sites of bonding. The energy gap (E_{HOMO}-E_{LUMO}) is a considerable stability index encourage the characterization of both kinetic stability and chemical reactivity of the molecules[54].

Molecules with a tinyenergy gap are considered soft molecules, they are highly polarized and more reactive than hard ones because they easily donate electrons. In Cu(II) complexes, the energy gap is very small exhibiting that the charge transfer easily occurs and affecting also the biological activity of the molecules. Furthermore, the entrance of some groups in conjugation resulting in the tiny values of energy gap [55].

DFT method concept, can indicate the chemical reactivity and site selectivity of the molecular systems. The energies of frontier molecular orbitals (E_{HOMO}+E_{LUMO}), energy band gap (E_{HOMO}- E_{LUMO})which illustrate the resultant charge transfer interaction within the molecules, electronegativity (χ), chemical potential (μ), global hardness (η), global softness (S) and global electrophilicity index (ω) [56,57] are listed in (Table 6).

3.8. Biological studies.

3.8.1. Antimicrobial activity

From the data obtained for diameter of inhibition zone (Table 7),it is clear that the ligand showed no activity against all bacterial strains. The complexes were selective as bacterial inhibitors on both types of bacterial strains. $[Cu_2(L\text{-}H)(OH)_2(C_2H_5O)(H_2O)]$ complex showed a remarkable antibacterial activitiy against all bacterial strains while $[Cu_2(L\text{-}H)_2(NO_3)_2]2H_2Oand[Cu_2(L\text{-}2H)SO_4(H_2O)_3]H_2O.1/2C_2H_5OH$complexes showed activity against only three bacterial strains(St. epid*; Strp. py.* and *Er*)compared with the standard drug (Ampicillin).On the other hand, $[Cu_2(L\text{-}2H)(L\text{-}H)(OAC)(H_2O)].4H_2O$exhibitedmoderate antibacterial activity against *Strp. py. o*nly. Such expanded action of the metal complexes can be clarified on the premise of the overtone idea and chelation hypothesis [58]. As indicated by the overtone concept of cell permeability, on chelation, the polarity of the metal ion is reduced to a great extent due to the overlap of the ligand orbital and the partial sharing of the positive charge of the metal ion with donor groups which increases the delocalization of electrons over the whole chelate ring and enhances the lipophilicity of the complex. Consequently, enhances the penetration of the complex into the lipid membrane and blocks the metal binding sites on the enzymes of the microorganism.

3.8.2. Scavenging activities of superoxide radicals

Superoxide dismutase (SOD) is the first line of vindication against injury caused by reactive oxygen species (ROS), which catalyze the dismutation of O^{-2} to H_2O_2, and O_2 [59]. Therefore, It is important to find SOD mimics, which have SOD activity and provide stability. This work focused on the metal dependent SOD mimics, their assays, chemical characters and usage. H_2L and its metal complexes were screened for their superoxide-scavenging activity in the PMS/NADH–NBT system, and the results are represented in Table8. In this system, superoxide anion derived from dissolved oxygen by PMS/NADH coupling reaction reduces NBT. The decrease of absorbance at 560 nm with antioxidant activities of the complexes indicates the consumption of superoxide anion in the reaction mixture. There is an apparent variation in the overall scavenging ability among the parent ligand and its metal complexes. $[Cu_2(L\text{-}H)(OH)_2(C_2H_5O)(H_2O)]$ has the potent activity comparable to ascorbic acid followed by the ligand displaying 67.6 % scavenging activities of the superoxide radical. On the other hand, other Cu(II) complexes revealed activity lower than 50%. Superoxide is a major factor in radiation damage, inflammation and tumor promotion. Fortunately, the present study has evolved a defense system against the toxicity of $O_2^{\bullet -}$ by the ligand and one of its Cu(II) complex.

***T*able 1: Elemental analysis and physical data of H_2TBAH and its Cu(II)complexes**

Compound	Mol.wt	Color	Found (calc.)%				M.p ◦C
			C%	H%	N%	M%	
H_2TBAH $C_{18}H_{18}N_4O_2S$	354.41	White	60.85 (60.99)	5.00 (5.12)	15.65 (15.80)	-	150
$[Cu_2(L\text{-}H)(OH)_2(C_2H_5O)(H_2O)]$ $Cu_2C_{20}H_{26}N_4O_6S$	578.30	Orange	41.75 (41.54)	4.13 (4.53)	9.12 (9.68)	21.85 (21.97)	195
$[Cu_2(L\text{-}2H)(L\text{-}H)(OAC)(H_2O)]4H_2O$ $Cu_2C_{38}H_{46}N_8O_{11}S_2$	982.00	Olive green	47.42 (46.47)	4.58 (4.72)	11.00 (11.40)	12.88 (12.94)	245
$[Cu_2(L\text{-}H)_2(NO_3)_2]2H_2O$ $Cu_2C_{36}H_{38}N_{10}O_{12}S_2$	993.91	Brown	44.87 (43.50)	4.07 (3.85)	13.75 (14.08)	12.97 (12.78)	208
$[Cu_2(L\text{-}2H)SO_4(H_2O)_3]H_2O.1/2C_2H_5OH$ $Cu_2C_{19}H_{27}N_4O_{10.5}S_2$	670.63	Brown	34.48 (34.02)	4.46 (4.05)	7.79 (8.35)	18.40 (18.95)	200

Table 2: IR spectral data of H_2TBAH and its Cu(II) complexes

Compound	ν (OH)	ν (NH)	ν *(C=O)*	ν (C=N)	ν (C-O)	N (N-N)	ν (C-S)	ν (M-O)	ν (M-N)
H_2TBAH	3450, 3435	3210, 3239	1668	1551	1176	1063	690	-	-
$[Cu_2(L\text{-}H)(OH)_2(C_2H_5O)(H_2O)]$	3450, 3422	3233	1659	1549	1164	1070	692	509	474
$[Cu_2(L\text{-}2H)(L\text{-})(OAC)(H_2O)]4H_2O$	3435, 3425	3225	1662(w)	1543	1131	1032	692	561	438
$[Cu_2(L\text{-}H)_2(NO_3)_2]2H_2O$	3433, 3423	3243	1666	1548	1138	1064	691	544	435
$[Cu_2(L\text{-}2H)SO_4(H_2O)_3]H_2O.1/2C_2H_5OH$	3433, 3423	3254	1658	1547	1113	1057	689	548	424

Table 3: Summary of electronic spectral data and magnetic moment

Compound	Band position, (Cm^{-1})	μeff(B.M)
H_2TBAH	35714, 32258, 25380, 20920	-
$[Cu_2(L\text{-}H)(OH)_2(C_2H_5O)(H_2O)]$	27932, 22624, 17857	1.67
$[Cu_2(L\text{-}2H)(L\text{-}H)(OAC)(H_2O)]4H_2O$	27777, 24038, 15150	1.53
$[Cu_2(L\text{-}H)_2(NO_3)_2]2H_2O$	27807, 22831, 21186, 19920, 18115	1.59

Table 4: Decomposition steps along with temperature range °C, removed species and weight loss(%) of H_2TBAH and its Cu(II) complexes

Compound	Temperature range, °C	Removed species	*Weight loss*	
			found	*Calc.*
H_2TBAH	114-264	$-2C_6H_{5+}N_{2+}2CN+4H_2$	68.45	68.42
	265-494	$-SO_2$	17.73	18.09
	495-800	-4 C (residue)	13.85	13.57
$[Cu_2(L\text{- }H)(OH)_2(C_2H_5O)(H_2O)]$	146-245	$-2C_6H_{5+}H_2O + C_2H_5OH$	37.45	37.57
	246-583	$-4HCN+ C_2H_{4+}SO$	31.9	31.85
	584-705	$-H_2O$	3.2	3.11
	706-800	-2CuO (residue)	27.35	27.5
$[Cu_2(L\text{-}2H)(L\text{-}H)(OAC)(H_2O)]4H_2O$	17-141	$-4H_2O$	7.30	7.34
	142-230	$-4\ C_6H_{5+}H_2O$	32.97	33.24
	231-282	$-4HCN +2N_2$	16.01	16.7
	283-563	$-CH_3COOH+ 2CO+ 2H_2$	12.5	12.23
	564-714	$-2CO+ C_2H_4$	8.19	8.56
	715-800	-2CuS + 2C (residue)	22.9	21.89
$[Cu_2(L\text{-}H)_2(NO_3)_2]2H_2O$	15-116	$-2H_2O$	3.770	3.62
	117-232	$-4\ C_6H_5+2NO$	37.51	37.06
	233-358	$-4CN+ 2N_{2+}7H_2$	17.5	17.5
	359-449	-4 CO	10.41	11.27
	450-712	-2 SO	9.69	9.67
	712-800	-2CuO + 4 C (residue)	21.11	20.84
$[Cu_2(L\text{-}2H)SO_4(H_2O)_3]H_2O.1/2C_2H_5OH$	18-131	$-H_2O+1/2C_2H_5OH$	6.3	6.12
	132-223	$-2C_6H_{5+}3H_2O+2HCN$	39.23	39.11
	224-444	$-SO_2$	9.37	9.55
	445-726	$-2NH_{3+}O_2$	9.76	9.84
	727-800	2CuO + S + 4C (residue)	35.33	35.66

Table 5: XRD data of the main 8 peaks$[Cu_2(L\text{- }H)(OH)_2(C_2H_5O)(H_2O)]$ex

2θ(degree)	15.02	17.92	20.68	24.76	28.44	43.98	64.26	77.40
d(A°)	5.89	4.94	4.29	3.59	3.13	2.06	1.45	1.23
Crystallite size *D*(nm)	33.48	56.03	35.16	21.79	57.09	47.12	30.63	39.39
FWHM	0.25	0.15	0.24	0.39	0.15	0.19	0.32	0.27
Lattice strain(ε)	0.0083	0.0042	0.0057	0.0078	0.0026	0.0021	0.0022	0.0015
% peak intensity	164	436	202	298	194	188	130	128

Table 6:Calculated E_{HOMO}, E_{LUMO}, energy band gap ($E_H - E_L$), chemical potential (μ), electronegativity(χ), global hardness (η), global softness (S), global electrophilicity index (ω) and softness(σ)for H_2TBAH and its Cu(II) complexes

Compound	E_H (eV)	E_L(eV)	(E_H-E_L) (eV)	χ (eV)	μ (eV)	η (eV)	S (eV^{-1})	ω (eV)	σ (eV^{-1})
H_2TBAH	-5.156	-2.538	-2.618	3.847	-3.847	1.309	0.382	5.653	0.764
$[Cu_2(L\text{- }H)(OH)_2(C_2H_5O)(H_2O)]$	-3.757	-3.026	-0.731	3.391	-3.391	0.365	1.368	15.735	2.736
$[Cu_2(L\text{-}2H)(L\text{-}H)(OAC)(H_2O)]4H_2O$	-3.448	-2.353	-1.095	2.900	-2.900	0.547	0.913	7.683	1.826
$[Cu_2(L\text{-}H)_2(NO_3)_2]2H_2O$	-3.729	-3.123	-0.606	3.426	-3.426	0.303	1.650	19.369	3.300
$[Cu_2(L\text{-}2H)SO_4(H_2O)_3]H_2O.1/2C_2H_5OH$	-3.445	-3.121	-0.324	3.283	-3.283	0.162	3.086	33.265	6.173

Table 7: Activity index of H_2TBAH and its Cu(II) complexes on Staphylococcus epidermid, streptococcus pyagenies,Erwinia andklebsiella Spp

Compound	*staph (mg/ml)*	*strepto (mg/ml)*	*Erwinia (mg/ml)*	*Klebsiella (mg/ml)*
	Diameter of inhibition zone (in mm)	Diameter of inhibition zone (in mm)	Diameter of inhibition zone (in mm)	Diameter of inhibition zone (in mm)
H_2TBAH	-ve	-ve	-ve	-ve
$[Cu_2(L\text{- }H)(OH)_2(C_2H_5O)(H_2O)]$	10.5	11	9	8
$[Cu_2(L\text{-}2H)(L\text{-}H)(OAC)(H_2O)]4H_2O$	-ve	6.5	-ve	-ve
$[Cu_2(L\text{-}H)_2(NO_3)_2]2H_2O$	8.5	9.5	7.5	-ve
$[Cu_2(L\text{-}2H)SO_4(H_2O)_3]H_2O.1/2C_2H_5OH$	7	6.5	7	-ve

Table 8: SOD like activity of H_2TBAH and its Cu(II) complexes

Sample	Δ through 5 min	% inhibition
Control	0.435	0%
L-Ascorbic acid	0.086	82.2%
H_2TBAH	0.141	67.6%
$[Cu_2(L\text{- }H)(OH)_2(C_2H_5O)(H_2O)]$	0.093	78.6%
$[Cu_2(L\text{-}2H)(L\text{-}H)(OAC)(H_2O)]4H_2O$	0.372	14.5%
$[Cu_2(L\text{-}H)_2(NO_3)_2]2H_2O$	0.353	18.8%
$[Cu_2(L\text{-}2H)SO_4(H_2O)_3]H_2O.1/2C_2H_5OH$	0.404	7.1%

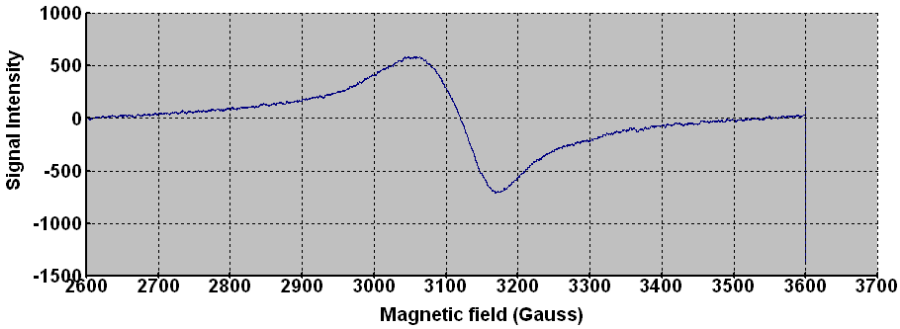

Fig.1: X-band ESR spectrum of $[Cu_2(L\text{-}H)_2(NO_3)_2]2H_2O$

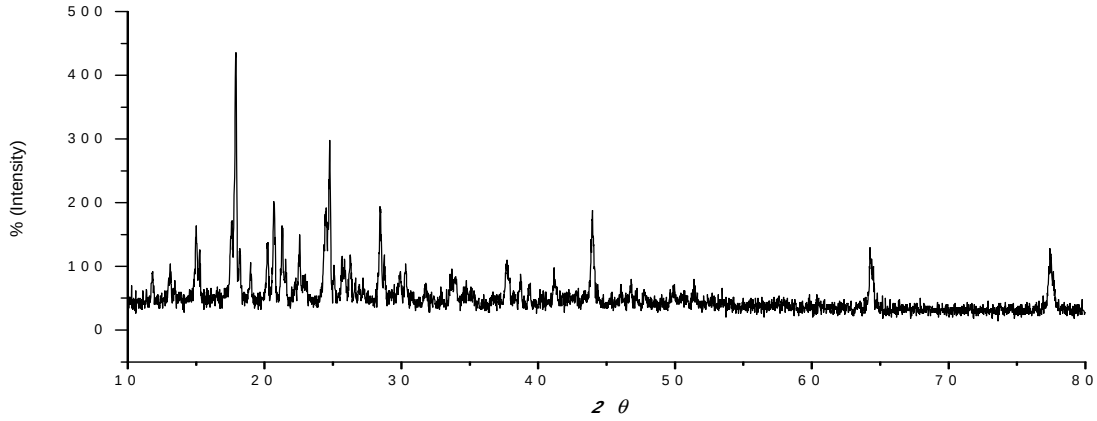

Fig.2: X-ray diffraction pattern of $[Cu_2(L\text{-}H)(OH)_2(C_2H_5O)(H_2O)]$

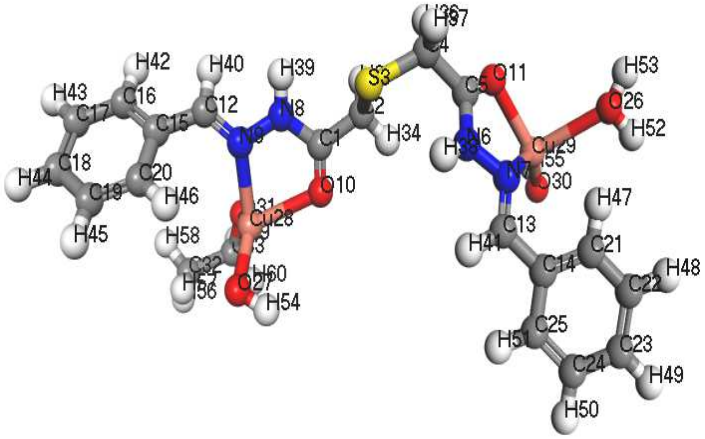

Structure 2: Molecular modelling of $[Cu_2(L\text{-}H)(OH)_2(C_2H_5O)(H_2O)]$

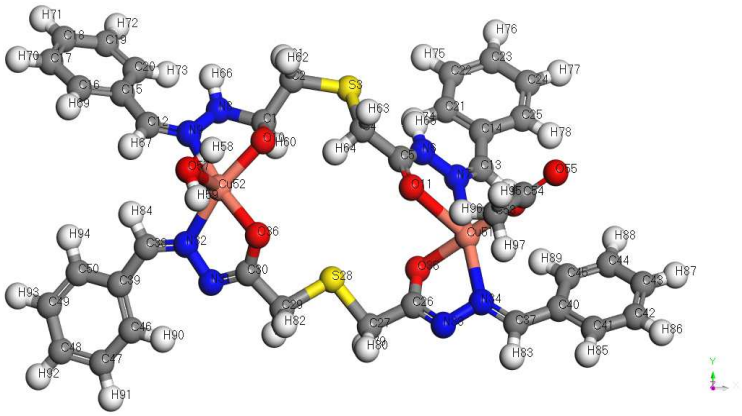

Structure 3: Molecular modeling of $[Cu_2(L\text{-}2H)(L\text{-}H)(OAC)(H_2O)]4H_2O$

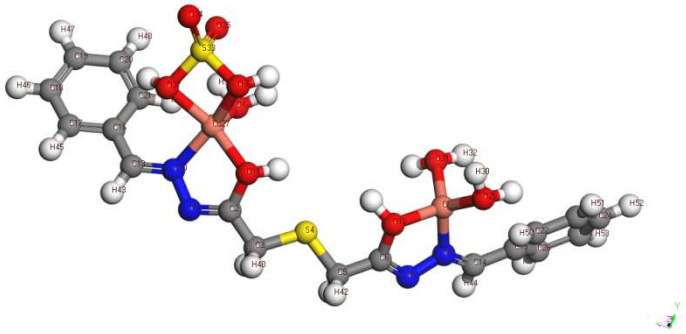

Structure 4: Molecular modeling of $[Cu_2(L\text{-}2H)SO_4(H_2O)_3]H_2O.1/2C_2H_5OH$

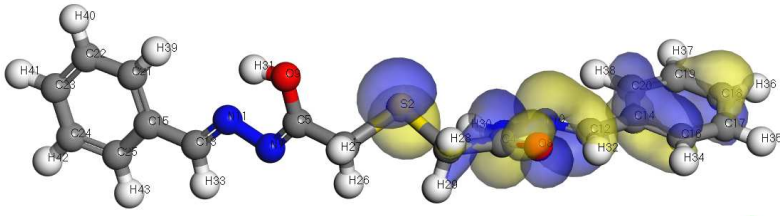

E_{LUMO}**= -2.538** ***eV***
(excited state)

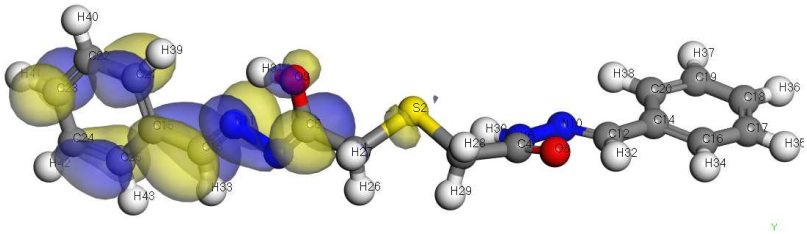

E_{HOMO}**= -5.156***eV*
(ground state)

Fig 3. 3D plots frontier orbital energies using DFT method for H_2TBAH

CONCLUSION

A series of metal (II)complexes of 2,2'-thiobis(N-benzylidene)acetohydrazide)(H_2L) has been prepared and characterized. A square planar, square pyramidal and octahedral geometries were suggested for the prepared complexes. Moreover, the ligand and its complexes were screened for antibacterial and antioxidant activities. While, the ligand was inactive towards the tested microorganisms, its Cu complexes showed acceptable antibacterial

activities. Structure activity relationship analysis showed that the geometry of the complexes has a significant effect on the extent of the biological activity ,as the square planar $[Cu_2(HTBAH)(OH)_2(C_2H_5O)(H_2O)]$ complex with the lowest coordination number, showed the strongest antibacterial and antioxidant activities.

REFERENCES

[1] S. Rollas and Ş.G.Küçükgüzel; *Molecules*,**2007**,12,1910-1939.
[2] P.Vicini, M. Incerti , I.A.Doytchinova, I.A. Doytchinova, P. L. Colla, B. Busonera, R.taLoddo, *Eur.J.Med.Chem*.,**2006**,41,624-632.
[3] C.Pelizzi, G.Pelizzi, F.Vitali, *J. Chem. Soc., Dalton Trans*., **1987**,177-181.
[4] A.Mangia , C.Pelizzi, G. Pelizzi , *Acta. Crystallogr. B*, **1974**, 30, 2146-2150.
[5] C.Pelizzi, G.Pelizzi, G.Predieriand, S. Resola *J. Chem.Soc*., *Dalton Trans*.,**1982**,1349-1354.
[6] M.B.Hursthouse,S. Amarasiri , A.Jayaweera , A. Quick, *J. Chem. Soc., Dalton Trans*., **1979**,279-282.
[7] R.Haran ,J. Gairinand and G.Commenges, *Inorg. Chim.Acta*,**1980**, 46, 63-67.
[8] J.Gómez , N.Leiva ,R. Arancibia, J. Oyarzo, G. E. Buono-Core, A. H. Klahn, V. Artigas, M. Fuentealba, R. Bosque, G. Aullón, C. López, M. Font-Bardía, T. Calvet,*Organomet. Chem*., **2016**, 819: 129-137.
[9] P. Paciorek, J.Szklarzewicz ,A. Jasińska, B. Trzewik, W. Nitek, M. Hodorowicz , Polyhedron, 2015, 17:226-232.
[10] G.Kumar, S.Devi, D. Kumar, *J. Mol. Struct.* , **2016**, 1108,680–688.
[11] V.S.Nogueira, M.Clara, R.Freitas, W.S. Cruz, T.S. Ribeiro, J. A.L.C. Resende, N. A. Rey, *J. Mol. Struct.*, **2016**,1106,121-129.
[12] A.H.Ahmed, A.M.Hassan,H.A. Gumaa, B. H. Mohamed, A. M. Eraky, A. A. Omran ,*Arab.J. Chem.*,**2016**, in press.
[13] R.Borthakura., A. Kumar and R.A.Lala; *Spectrochim. Acta, Part A: Molecular and Biomolecular Spectroscopy*, **2015**,149, 621–629.
[14] A. E. M., El-Sayed, O.A.Al-Fulaij, A.A.Elaasar, M.M. El-Defrawy, A.A. El-Asmy, *Spectrochim. Acta, Part A: Molecular and Biomolecular Spectroscopy*, **2015**, 135, 211–218.
[15] D.P.Singh, B.K. Allam , K.N.Singh, V. P. Singh, *J. Mol. Catal. A: Chem*., **2015**, 398,158–163.
[16] B. Jeragh and A.A.El-Asmy; *Spectrochimic. Acta Part A: Molecular and Biomolecular Spectroscopy*, ,**2014**, 125: 25–35.
[17] V.Getautis , M.Daskeviciene , T.Malinauskas, V. Jankauskas, J. Sidaravicius, *Thin. Solid Films*, **2008**, 516,8979-8983.
[18] H. J. C.Bezerra-Netto, D.I.Lacerda, A. L. P. Miranda et al; *Bioorg.Méd.Chem*.**2006**, 14, 7924–7935.
[19] O.A.El-Gammal,E.A. Elmorsy and Y.E.Sherif, *Spectrochim. Acta, Part A: Molecular and Biomolecular Spectroscopy*, **2014**, 120, 332-339.
[20] O.Pouralimaradan, A.C. Chamayou, C.Janiak et al, *Inorg. Chim. Acta*.**2007**, 360,1599-1608.
[21] M.Bakir , O.Green and W.H.Mulder*; J.Mol.Struct*, **2008**, 873,17-28
[22] M.Alagesan, N. S. P. Bhuvanesh and N.Dharmaraj; *J. Chem. Soc.(* Dalton trans), **2013**, 42, 7210-7223.
[23] M.Shebl, M.A. El Ghamry, S.M.Khalil; *Spectrochimic. Acta Part A: Molecular and Biomolecular Spectroscopy*, **2014**, 126,232-241.
[24] Z. H. Chohan and M.A.Farooq, *Synth. React. Inorg. Met.-Org. Chem*. **2001**, 31,1853-1871.
[25] Z. H. Chohan, M. Praveen and S. K. A. Sherazi., *Metal-based Drugs*, **1998**, 5, 267-274.
[26] M. Płotek M., K.Dudek and A.Kyzioł, Chemik, **2013**, *Chemik*, 67, 12, 1181–1190.
[27] H.Zimmer, E. Shaheen , *J. Org. Chem*. 24,**1959**, 1140-1141.
[28] B. Delley, *Phys. Rev.B Condens.Matter*, **2002**, 66, 155125-155129.
[29] "Modeling and Simulation Solutions for Chemicals and Materials Research", Materials Studio, Version 7.0, Accelrys software Inc., San Diego, USA (**2011**).
[30] W. J.Hehre, " Ab initio molecular orbital theory", Wiley-Interscience, **1986**.
[31]A. Kessi and B.Delley; *Int. J. Quantum Chem*.,**1998**,68,135-144.
[32] A.Matveev , M.Staufer,M. Mayer; *Int. J. Quantum Chem*. **1999**, 75:863-873.
[33] B.Hammer, L.B.Hansen and J.K.Nørskov; *Phys. Rev. B:Condens. Matter*,**1999**, 59,7413-7421.
[34] I.Ahmad and A.Z.Beg , *J. of ethnopharmacol* , **2001**, 74,113-123.
[35]O.A. El-Gammal, *Inorgan. Chim. Acta*.,**2015**, 435:73–81.
[36] S.M. Bridges and M.L.Salin; *Plant Physiol*.,**1981**, 68, 275-278.
[37] W.J. Geary; *Coord. Chem. Rev*.,**1971**, 7,81-122.
[38] O. A. El-Gammal, G. A. El-Reash and S. F. Ahmed; *J. Mol. Struct*., **2012**,1007,1-10.
[39] O. A. El-Gammal, G.A.El-Reash and M.El-Gami, *Spectrochim. Acta Part A: Molecular and Biomolecular Spectroscopy*, **2012**, 96,444-455.
[40] K. Nakamoto" Infrared Spectra of Inorganic and Coordination Compounds", 3rd Edn., Wiley, New York, 1970.
[41] K.Chanda., P.K.Sharma and B.S. Gray*; J. Inorg. Nucl.Chem*. **1980**, 42,187-193.
[42] H.M.El-Shaaer, P.Foltfnova and M.Lacova; *Farmaco*.**1998**, 53, 224-232.

[43] O.A.El-Gammal, G.M.Abu El-Reash and M.El-Gamil, *Spectrochim. Acta Part A: Molecular and Biomolecular Spectroscopy*, **2014**, 123: 59 -70.
[44] A. B. P. Lever" Inorganic electronic spectroscopy. Amsterdam, The Netherlands: Elsevier. 420 p, **1968**.
[45]O.A. El-Gammal, M.M.Bekheit and Mai Tahoon; *Spectrochim. Acta, Part* A, **2015**, 135,597-607.
[46] K.Y Choi, M. J.Kim and D.S.Kim, *Bull. Korean Chem. Soc*., **2002**, 23, 1062-1066.
[47] O.A.El-Gammal, G.M.Abu El-Reash and S.A. Ahmed; *Spectrochim. Acta Part A: Molecular and Biomolecular Spectroscopy*, **2015**, 135, 690–703.
[48] M.Mohan and M. Manmohan., *Synth.React.Inorg.Met.-Org.Chem*., **1982**, 12: 761-784.
[49] F.A. El-Sayed, A.M. Donia and S.M.Hamza, *Thermochim. Acta*, **1991**, 189: 297-311.
[50] R.C.Maurya, D.D.Mishra, S.K.Jaiswal; R.C; *Synth. React. Inorg. Met.-Org.Chem*., **1995**, 25, 521-535.
[51] O. A. El-Gammal; *Spectrochim. Acta Part A: Molecular and Biomolecular Spectroscopy*, **2010**, 75: 533-542.
[52] A. A. R. Despaigne , J. G. Da Silva and A. C. M. Do Carmo, *J. Mol. Struct*, **2009**, 920:97-102.
[53] O.A.El-Gammal , I. M El-Mehasseb, R. H. Salama and G.M.Abu El-Reash, *Int.J.Adv. Res. Biol. Sci.* ,**2016**, 3, 263-282.
[54] M.Govindarajan, S.Periandy and K.Carthigayen, *Spectrochim. Acta Part A: Molecular and Biomolecular Spectroscopy*, **2012**, 97, 411-422.
[55] G.M.Abu El-Reash, O.A. El-Gammal, S.Ghazy and A.Radwan, *Spectrochim. Acta Part A: Molecular and Biomolecular Spectroscopy*, **2013**, 104: 26-34.
[56]R.G. Pearson; *J.Org. Chem*.,**1989**, 54:1423-1430.
[57] J. Padmanabhan, R. Parthasarathi, V.Subramanian, . *J. Phys. Chem. A.*, **2007**, 111, 1358-1361.
[58] N.Raman, V.Muthuraj, S.Ravichandran, *Proc. Ind. Acad. Sci*., **2003**, 115,161-167.
[59] L.A.del Río, f.J.Corpas, l.M. Sandalio, *J. Exp. Bot*. , **2002**, 53:1255-1272.